

PAPER • OPEN ACCESS

Polyacrylonitrile nanofiber as polar solvent N,N-dimethyl formamide sensor based on quartz crystal microbalance technique

To cite this article: A Rianjanu *et al* 2018 *J. Phys.: Conf. Ser.* **1011** 012067

View the [article online](#) for updates and enhancements.

You may also like

- [Electrochemical Determination of Sunitinib in Biological Samples Using Polyacrylonitrile Nanofibers/Nickel-Zinc-Ferrite Nanocomposite/Carbon Paste Electrode](#)
Ali Yarahmadi, Tayyeb Madrakian, Abbas Afkhami et al.
- [Electrospun graphene oxide incorporated PAN nanofibers, before and after activation](#)
Golchin Ghaderi, Hossein Tavanai and Mehdi Bazarganipour
- [Electrospun PAN-HNTs composite nanofiber membranes for efficient electrostatic capture of particulate matters](#)
Shiqian Hu, Ruowang Chen, Peng Lu et al.



ECS
The
Electrochemical
Society
Advancing solid state &
electrochemical science & technology

DISCOVER
how sustainability
intersects with
electrochemistry & solid
state science research

Polyacrylonitrile nanofiber as polar solvent N,N-dimethyl formamide sensor based on quartz crystal microbalance technique

A Rianjanu¹, T Julian¹, S N Hidayat¹, E A Suyono³, A Kusumaatmaja^{1,2}, and K Triyana^{1,2}

¹ Department of Physics, Universitas Gadjah Mada Sekip Utara Yogyakarta, 55281, Indonesia

² Nanomaterial Research Group, Universitas Gadjah Mada Sekip Utara Yogyakarta, 55281, Indonesia

³ Department of Biology, Universitas Gadjah Mada Sekip Utara Yogyakarta, 55281, Indonesia

aditya.rianjanu@mail.ugm.ac.id

Abstract. Here, we describe an N,N-dimethyl formamide (DMF) vapour sensor fabricated by coating polyacrylonitrile (PAN) nanofiber structured on quartz crystal microbalance (QCM). The PAN nanofiber sensors with an average diameter of 225 nm to 310 nm were fabricated via electrospinning process with different mass deposition on QCM substrate. The nanostructured of PAN nanofiber offers a high specific surface area that improved the sensing performance of nanofiber sensors. Benefiting from that fine structure, and high polymer-solvent affinity between PAN and DMF, the development of DMF sensors presented good response at ambient temperature. Since there is no chemical reaction between PAN nanofiber and DMF vapour, weak physical interaction such absorption and swelling were responsible for the sensing behavior. The results are indicating that the response of PAN nanofiber sensors has more dependency on the nanofiber structure (specific surface area) rather than its mass deposition. The sensor also showed good stability after a few days sensing. These findings have significant implications for developing DMF vapour sensor based on QCM coated polymer nanofibers.

Keywords: polyacrylonitrile (PAN), nanofiber, quartz crystal microbalance (QCM), N,N-dimethyl formamide (DMF), vapour sensing

1. Introduction

Polar organic solvent such N,N-dimethyl formamide (DMF) are widely used the chemical in various industries, such as the production of synthetic fibers, films, and coatings, and leather tanning [1]. Recent studies have suggested its serious health concerns that associated with exposure to DMF vapor through skin contact and inhalation. Many studies show the effect of DMF vapor both on exposed worker [2] and animal experiments [3] have confirmed the hepatotoxicity of DMF. The other experiment suggested embryotoxicity [4] and carcinogenesis [5] effect due to exposure to DMF vapors. Because of the health-related issues and the widespread use in industry, DMF has been



prioritized for field study. The detection and standard sampling for DMF vapor in the air require lengthy and complicated procedures and the use of gas chromatography (GC) [6]. Therefore an efficient, selective, and convenient sensor for DMF vapor is desirable.

Recently, various vapor sensors have been produced by using different sensing materials, such as inorganic thin films [7,8], semiconductor metal oxides [9,10], and conducting polymers [11] with excellent sensitivity results. Various vapor sensor was also have been developed based on different sensing mechanisms such as photoelectric sensors [12], resistance sensor [13], optical sensor [14], amperometric sensor [15] and acoustic wave sensor [15]. Quartz crystal microbalance (QCM) is one example of acoustic wave (AW) sensor platform based on acoustic-electric effect and mass deposition. A QCM sensor offers an accurate, real-time detection, and suitable sensors with high sensitivity response that is widely used as vapor/gas sensors [16]. Nanostructure material especially nanofibers have received increasing attention for various applications including gas sensor application due to their large specific surface area, high porosity and interconnected porous structures [17-19]. Many researchers have been used electrospun nanofiber [20,21] and polymer modified nanofiber [16,22] as sensing layer for various vapor/gas sensing.

The sensing mechanism of vapor sensor mainly dominated by chemical interaction between the active layer and the analytes. However, many volatile organic compounds like methanol, benzene, and toluene are not reactive at room temperature and mild conditions; fortunately, they may have weak physical interactions with the sensing layer, involving absorbing or swelling the polymer matrices. These interactions do not change the oxidation levels of conducting polymers, although, can also affect the properties of the sensing layer and make these vapor/gases detectable [23]. Several studies have been done investigating the swelling behavior of various polar solvent at electrospun nanofiber membrane to improve their electrical or mechanical properties [24-27]. Huang et al. (2013) investigated the swelling effect of polyacrylonitrile (PAN) and polysulfone (PSU) nanofiber after solvent vapor treatment with N,N-dimethyl formamide. The results confirmed that swelling behavior occurred when PAN nanofiber was exposure with DMF. The swelling behavior of PAN nanofiber and DMF vapor is expected due to their high polymer-solvent affinity. Based on their results, we are developing an N,N-dimethyl formamide (DMF) sensor based on polyacrylonitrile (PAN) nanofiber as sensing layer. We suspected that the weak physical interaction including absorption and swelling phenomena between PAN nanofiber and DMF vapor is responsible for DMF sensing.

2. Experimental

Typical Polyacrylonitrile (PAN) with a molecular weight of 150,000 from Sigma-Aldrich was used for the preparation of nanofiber. Non-ionic surfactant Triton x-100 was purchased from Merck, Germany. The solvents used for dissolving PAN and vapor sensing N, N-dimethyl formamide (DMF) was purchased from Merck, Germany. AT-Cut QCM sensor with the gold electrode and 10 MHz resonant frequency were purchased from Novaetech, Italy. All above materials used as received without any further purification.

Polyacrylonitrile (PAN) nanofiber was prepared by dissolving 0.5 g and 0.6 g polymer PAN into 10 mL DMF followed by mechanical stirring at 1000 rpm for 24 hours at ambient temperature until a homogeneous solution was achieved. After PAN fully dissolved in DMF, a small amount (1%) of non-ionic surfactant Triton X-100 was added to the solution. The non-ionic surfactant is added to lower the surface tension of the solution. Followed by mechanical stirring at 900 rpm for 30 min to fully dissolve the surfactant.

The solution then transferred into 10 mL plastic syringes for electrospinning process. When the electrospinning process was performed, a DC voltage of 5 kV and 10 kV was applied, and the tip to collector distance was set as 10 cm. The collector used in the electrospinning process was metal plate covered with aluminum foil with crystal QCM put in the collector. The electrospinning process was carried out for 30 s to get a suitable thickness nanofiber film. Finally, the nanofiber film was placed in the desiccator for 12 hours to evaporate the residual solvent before further treatment. To vary the nanofiber morphology, we used a different parameter in electrospinning process. Detailed listed of

electrospinning parameter used in this study is listed in Table. 1. Scanning electron microscope (SEM) JEOL-JSM-6510 with auto fine coater JEOL JEC-3000FC was used for investigating the morphologies of electrospun nanofiber PAN.

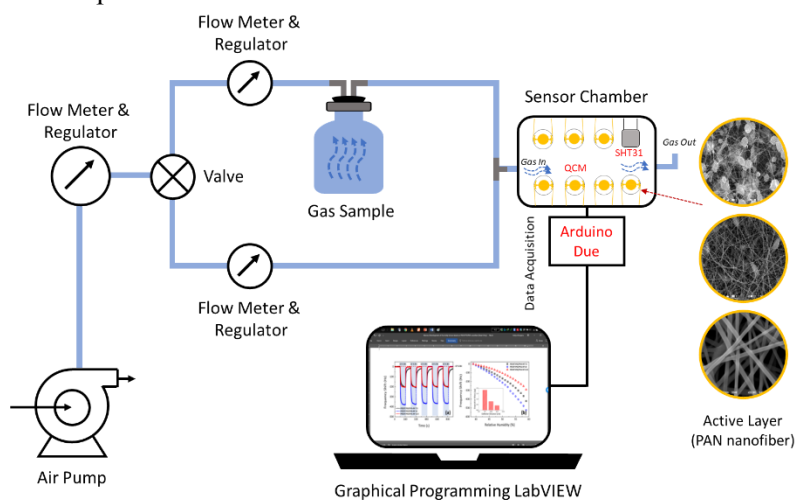


Figure 1. Schematic illustration of PAN nanofiber QCM vapor sensing process

A schematic diagram of the N,N-dimethyl formamide vapor sensing system is presented in Fig. 1. The QCM sensor was installed in the testing chamber with Sensirion SHT 31 (temperature and humidity sensor) included to monitoring the humidity and the temperature of the chamber. During the experiments process, several of gas flow rate was used. The sensing of the QCM sensor was measured by a shift in the resonance frequency. The shift in the resonance frequency is directly related to mass deposition on sensing layer according to Sauerbrey equations [28]. The resonance frequency sent to PC accompanies RS232 or serial protocol with graphical programming language LabVIEW.

3. Results and Discussion

The representative SEM image of the PAN nanofiber membrane used in this study is shown in Fig. 2. The as-spun nanofibers were randomly oriented three-dimensional structure (3D) porous structure with relatively random diameter varies from 225 nm to 310 nm. The electrospinning parameter was varying to obtain three different nanofiber morphologies. Several studies have been revealed that the sensitivity of gas sensors can be efficiently improved by increasing the specific surface area (SSA) per unit mass of the sensing layer. The specific surface area of smooth nanofiber is higher compared than the beaded fiber. However, the smooth nanofiber with higher diameter has lower specific surface area [29]. So, the optimum morphologies are a crucial aspect to improve the sensor sensitivity.

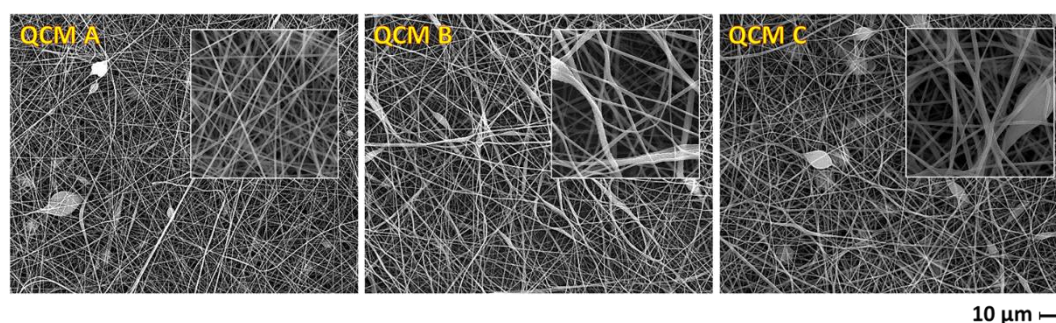


Figure 2. SEM image of PAN nanofiber with different electrospinning parameters

The parameter used and detailed nanofiber form with frequency shift after the deposition was shown in Table. 1. It shows that the frequency shift after coating increase from QCM A to QCM C. It

means that the mass deposition of nanofiber PAN in QCM substrate was also increasing. Fig. 3 shows the mass deposition and nanofiber diameter of PAN nanofiber sensors. The nanofiber diameter was found about 225 nm, 242 nm, and 310 nm for QCM A–C, respectively. The increase in the nanofiber diameter is due to the increased viscosity of the solution. The viscosity of the polymer solution directly depends on their solution concentration. In the electrospinning process, high viscosity solution means that the polymer chain bonding is high enough to maintain its shape thus make nanofiber with higher diameter.

Table 1. The parameter used in the electrospinning process with frequency shift after coating and nanofiber formation.

Sample	Electrospinning parameter (t = 20 s)			Frequency Shift after Coating (Hz)
	d (cm)	c (wt%)	V (kV)	
QCM A	10	5	5	1344
QCM B		10	10	2163
QCM C		6	5	4130

The correlation of frequency shift with mass deposition as mention before is described by Sauerbrey equations. We found that the mass deposition is about 296 ng, 476 ng, and 909 ng for QCM A–C, respectively. The difference in the mass deposition is due to the different deposition rate when the electrospinning process. The deposition rate of electrospinning process depends on the velocity of the polymer molecule under the influence of processing voltage. The increasing of processing voltage would increase the velocity of polymer molecules and make the deposition rate increased. Both nanofiber mass deposition and nanofiber diameter increase from QCM A to QCM C. The response of the QCM sensor is highly dependent on the change in humidity and usually utilized as humidity sensors [30]. Since the response of QCM sensor is highly dependence to the alteration of relative humidity; we also investigated the response of our sensor in the influence of relative humidity change. The linear correlation between humidity shift and frequency response of our sensor is shown in inset Fig. 3 (a). It shows that the correlation is about 2.17, 0.68, 1.96, and 2.72 Hz/%RH for uncoated (blank), QCM A, QCM B, and QCM C, respectively. The value is insignificant compared to the response of PAN nanofiber sensors, and being neglectable to the response measurement.

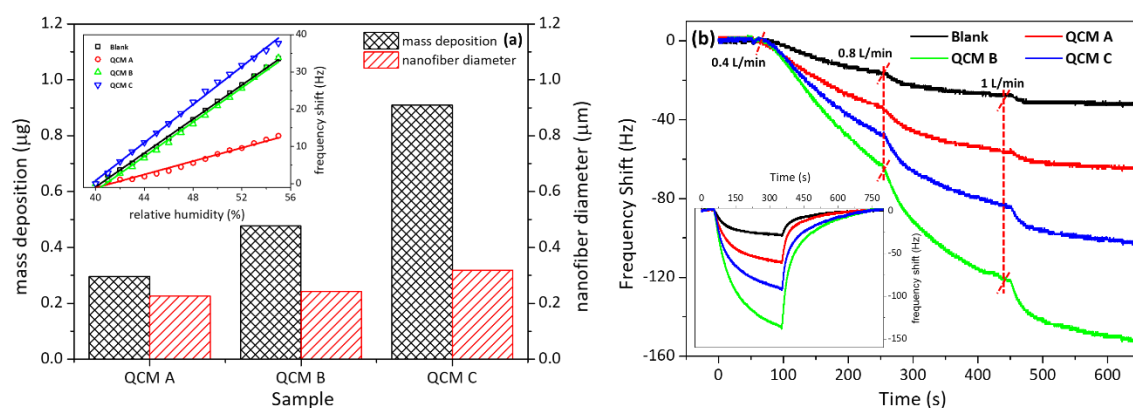


Figure 3. (a) Mass deposition and nanofiber diameter of PAN nanofiber QCM sensors (inset: humidity dependence of PAN nanofiber QCM sensors), (b) Dynamic response of QCM sensors coated with PAN nanofiber upon exposure to increasing the gas flow of DMF vapor, (inset: one cycle of QCM response against DMF vapor 1 L/min).

Fig. 3 (b) shows the dynamic response of PAN nanofiber QCM sensors with several of gas flow rate. It shows that the response is increasing consecutively from blank to QCM A, QCM C, and the highest response is achieved with QCM B. For commonly QCM sensors increasing mass deposition

would increasing its sensor sensitivity [22]. However, in our results, the highest response was achieved by QCM B which has lower mass deposition than QCM C. These results were occurred due to the higher specific surface area (SSA) that QCM B possessed. Jia et al. (2017) found that smooth nanofiber formation with larger diameter has lower specific surface area [29]. This particular reason is the causes of the higher response of QCM B. In our cases, the specific surface area of nanofiber sensor has more influence rather than its mass depositions. Inset Fig. 3 (b) shows the dynamic response (adsorption/desorption) of the sensor of PAN nanofiber sensors with 1 L/min gas flow rate. The results show that the response time is faster than its recovery time. The slow response time (over 300 s) is suspected due to the low evaporation rate of DMF solvent. The DMF solvent has a boiling point of 153 °C which makes the DMF solvent hardly to evaporate at ambient temperature.

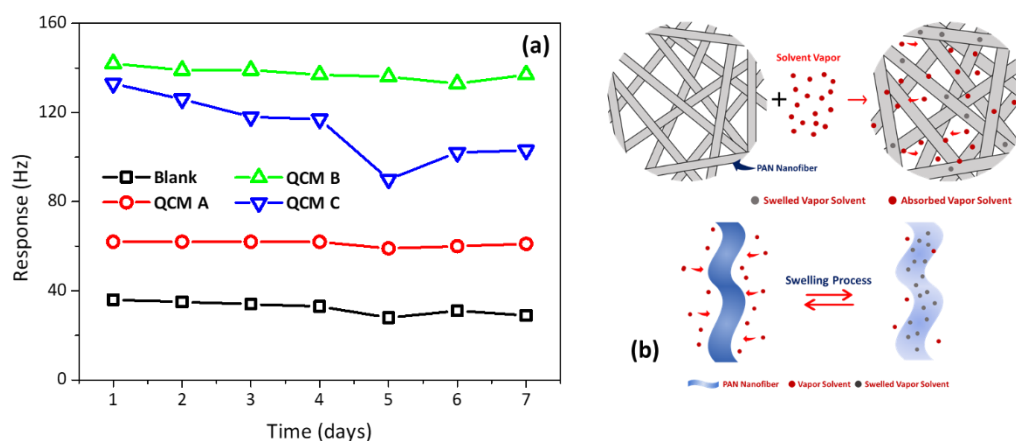


Figure 4. (a) Respons stability of PAN nanofiber QCM sensors with 1 L/min gas flow of DMF vapor, (b) Schematic illustration of sensing mechanism

We also investigated the stability of the response frequency of PAN nanofiber sensors under the influence of DMF vapour. Fig. 4 (a) shows the response of sensor after sensing DMF vapor with vapor flowrate 1 L/min. It shows that QCM C is quite unstable for one week used, while the other sample is relatively stable. This is probably due to beaded morphologies that QCM C possessed. The sensing mechanism of PAN nanofiber gas sensor under the influence of DMF vapour shows in Fig. 4 (b). We believe that the weak physical interaction such as absorption and swelling is responsible for the change in the resonance frequency. From Fig. 4 (b) we illustrated the phenomena that occurred after the PAN nanofiber exposure with DMF vapour. The DMF molecules are partly absorbed into the PAN nanofiber utilizing the high affinity between DMF molecules and PAN polymers via the swelling process. However, this mechanism alone couldn't deliver such high response. In addition to swelling behavior, we believe that the porous structure in PAN nanofiber film may contribute as a temporary shelter for DMF molecules and increase the mass loading of the active layer. Both phenomena in our belief are responsible for the change in the resonance frequency of the PAN nanofiber sensor under the influence of DMF vapour.

4. Conclusion

N,N-dimethyl formamide vapour sensor based on polyacrylonitrile nanofiber deposited on QCM substrate has been successfully developed. The increase in nanofiber specific surface area and its mass deposition increases the sensor sensitivity. The change in the resonance frequency of the sensing element upon exposure to DMF vapour is caused by weak physical interaction such as absorption and swelling of DMF molecules and into polyacrylonitrile nanofibers. The PAN nanofiber sensors show excellent stability in sensing DMF after one week.

Acknowledgment

This work was supported by the “Penelitian Pendidikan Magister Menuju Doktor Sarjana Unggulan (PMDSU), Contract No. 1991/UN1-P.III/DIT-LIT/LT/2017” from the Ministry of Research Technology and Higher Education, the Republic of Indonesia.

References

- [1] Li Y, Zhang S and Song D 2013 *Angewandte Chemie - International Edition* **52** 710–3
- [2] Long G and Meek M E 2001 *Journal of Environmental Science and Health, Part C* **19** 161–87
- [3] Rui D, Daojun C and Yongjian Y 2011 *Environmental Toxicology and Pharmacology* **31** 357–63
- [4] Saillenfait A M 1997 *Fundamental and Applied Toxicology* **39** 33–43
- [5] Senoh H, Aiso S, Arito H, Nishizawa T, Nagano K, Yamamoto S and Matsushima T 2004 *Journal of Occupational Health* **46** 429–39
- [6] Rimatori V and Carelli G 1982 *Scandinavian Journal of Work, Environment & Health* **8** 20–3
- [7] Kaushik A, Kumar R, Arya S K, Nair M, Malhotra B D and Bhansali S 2015 *Chemical Reviews* **115** 4571–606
- [8] Evans S D, Johnson S R, Cheng Y L and Shen T 2000 *Journal of Materials Chemistry* **10** 183–8
- [9] Dhahri R, Leonardi S G, Hjiri M, Mir L El, Bonavita A, Donato N, Iannazzo D and Neri G 2017 *Sensors and Actuators, B: Chemical* **239** 36–44
- [10] Hidayat S N and Triyana K 2016 *AIP Conference Proceedings* vol 1755p 20001
- [11] Bora A, Mohan K, Pegu D, Gohain C B and Dolui S K 2017 *Sensors and Actuators B: Chemical* **253** 977–86
- [12] Cui J, Wang D, Xie T and Lin Y 2013 *Sensors and Actuators B: Chemical* **186** 165–71
- [13] Wang J, He E, Liu X, Yu L, Wang H, Zhang R and Zhang H 2017 *Sensors and Actuators B: Chemical* **239** 898–905
- [14] Evyapan M, Kadem B, Basova T V., Yushina I V. and Hassan A K 2016 *Sensors and Actuators B: Chemical* **236** 605–13
- [15] He K, Wang X, Meng X, Zheng H and Suye S I 2014 *Sensors and Actuators, B: Chemical* **193** 212–9
- [16] Wang N, Wang X, Jia Y, Li X, Yu J and Ding B 2014 *Carbohydrate Polymers* **108** 192–9
- [17] Ding B, Wang M, Yu J and Sun G 2009 *Sensors* **9** 1609–24
- [18] Triyana K, Mu'min M S, Faizah K, Yusuf Y, Kusumaatmaja A and Harsojo S 2015 *Materials Science Forum* **827** 321–5
- [19] Kusumaatmaja A, Sukandaru B, Chotimah and Triyana K 2016 *AIP Conf. Proc.* 1755
- [20] Jia Y, Yu H, Zhang Y, Chen L and Dong F 2015 *Sensors and Actuators B: Chemical* **212** 273–7
- [21] Jia Y, Chen L, Yu H, Zhang Y and Dong F 2015 *RSC Adv.* **5** 40620–7
- [22] Huang W, Wang X X, Jia Y, Li X, Zhu Z, Li Y, Si Y, Ding B, Wang X X and Yu J 2013 *RSC Advances* **3** 22994–3000
- [23] Bai H and Shi G 2007 *Sensors* **7** 267–307
- [24] Huang L, Manickam S S and McCutcheon J R 2013 *Journal of Membrane Science* **436** 213–20
- [25] Chotimah, Rianjanu A, Winardianto B, Munir M, Kartini I and Triyana K 2016 *International Journal on Advanced Science, Engineering, and Information Technology* **6** 675–81
- [26] Liu C, Li X, Liu T, Liu Z, Li N, Zhang Y, Xiao C and Feng X 2016 *Journal of Membrane Science* **512** 1–12
- [27] Kusumaatmaja A, Fauji N, and Triyana K 2017 *Mater. Sci. Forum* 886 145–9
- [28] Sauerbrey G 1959 *Zeitschrift für Physik* **155** 206–22
- [29] Jia Y, Yu H, Cai J, Li Z and Dong F 2017 *Sensors and Actuators B: Chemical* **243** 1042–5
- [30] Hidayat SN, Julian T, Rianjanu A, Kusumaatmadja A, Triyana K and Roto 2017 *International Seminar on Sensors, Instrumentation, Measurement, and Metrology (ISSIMM) (IEEE)* 119–23.